Supporting Information for

High-resolution infrared spectroscopy and ASAP analysis of cyclopentadiene

The vibrational modes below 860 cm^{-1} and the ν_{21} mode at 961 cm^{-1}

Luis Bonah,[*,†] Marie-Aline Martin-Drumel,[‡] Olivier Pirali,[‡] Francesca Tonolo,[¶] Michela Nonne,[§] Mattia Melosso,[‖] Luca Bizzocchi,[‖] Cristina Puzzarini,[‖] Jean-Claude Guillemin,[⊥] Christian P. Endres,[#] Stephan Schlemmer,[†] and Sven Thorwirth[†]

†*I. Physikalisches Institut, Universität zu Köln, Zülpicher Str. 77, 50937 Köln, Germany*
‡*Institut des Sciences Moleculaires d'Orsay, Université Paris Saclay, 598 Rue André Rivière, 91400 Orsay, France*
¶*Univ. Rennes, CNRS, IPR (Institut de Physique de Rennes), UMR 6251, 35000 Rennes, France*
§*Scuola Superiore Meridionale, Largo San Marcellino 10, 80138 Naples, Italy*
‖*Dipartimento di Chimica "Giacomo Ciamician", Università di Bologna, Via P. Gobetti 85, 40129 Bologna, Italy*
⊥*Univ. Rennes, Ecole Nationale Supérieure de Chimie de Rennes, ISCR-UMR 6226, 35000 Rennes, France*
#*The Center for Astrochemical Studies, Max-Planck-Institut für extraterrestrische Physik, Gießenbachstraße 1, 85748 Garching, Germany*

E-mail: bonah@ph1.uni-koeln.de

A GUI of the new ASAP implementation

Fig. S1 shows the graphical user interface (GUI) of the ASAP implementation in LLWP.[1] The Loomis-Wood plot for the $J_{15,J-15}$ series of target levels is shown in the center (the respective target levels are given in the top right corner of each plot). The target level series can be selected in the *ASAP Settings window* (top right). The $25_{15,10}$ level was just assigned as is indicated by the blue color of the target level in the right corner, the fitted lineshape in orange, and the assignment marker in pink. Determining the center position of this single cross-correlation peak results in the seven assignments that are shown in the *New Assignments* window on the bottom right. These are the position of the target level and the six transitions making up the cross-correlation plot, which are also highlighted in the *ASAP Detail Viewer* window on the left (similar to the right column of Fig. 2 of the main manuscript).

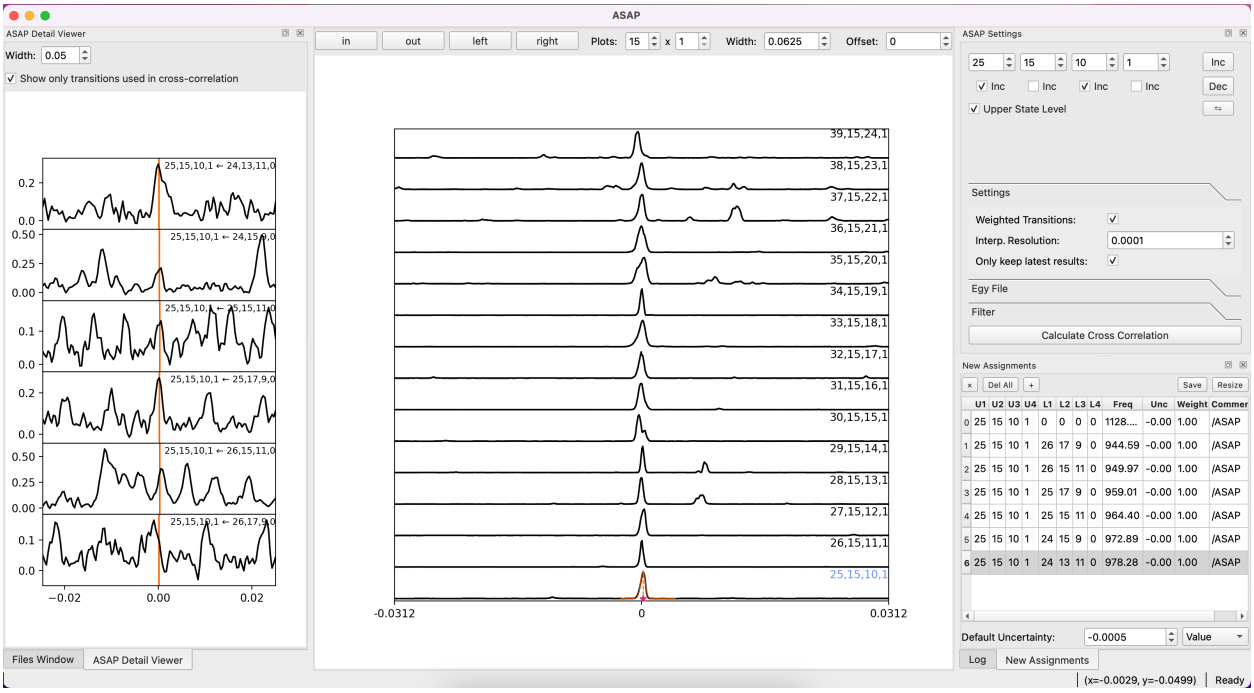

Figure S1: Graphical user interface of the ASAP implementation in LLWP.

Important settings can be found in the *ASAP Settings* window (top right). The interpolation resolution should be set similar to the experimental resolution. Too high values increase the computation time and too low values result in no or low-resolution cross-correlation peaks. The predictions should be filtered by intensity to exclude any transitions that are not visible in the spectrum. These settings can be found in the *Settings* and *Filter* tabs in the *ASAP Settings* window, respectively.

B Results of the ASAP^2 analysis

The ASAP^2 cross-correlation plots are presented for all measured bands: ν_{26}, ν_{27}, ν_{10}, and ν_{22} in Fig. S2 as well as $2\nu_{27}$, $\nu_{27}+\nu_{14}$, and $\nu_{27}+\nu_{14}-\nu_{14}$ in Fig. S3. In each figure, the number of cross-correlated lines n and the FWHM w are given. For the FWHM w, a Gaussian was fitted to the resulting ASAP^2 lineshape. Except for Fig. S2a, saturated lines (defined as lines where the intensity peaks above 0.9 within the shown window) were excluded for improved visual clarity. Differences in the cross-correlated lines n between the figures and the tables

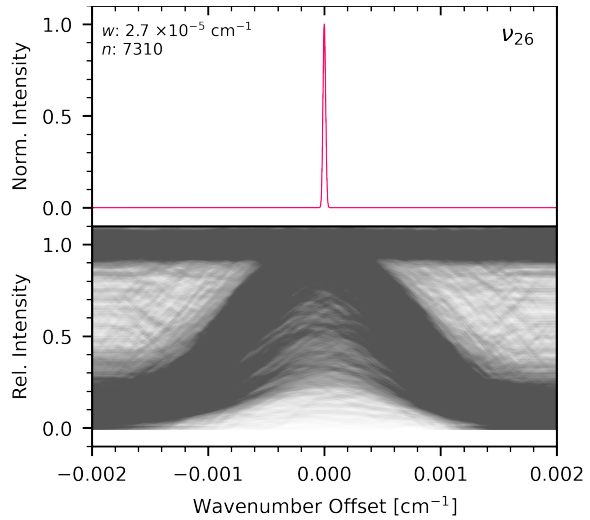

(a) ASAP^2 analysis for the ν_{26} band.

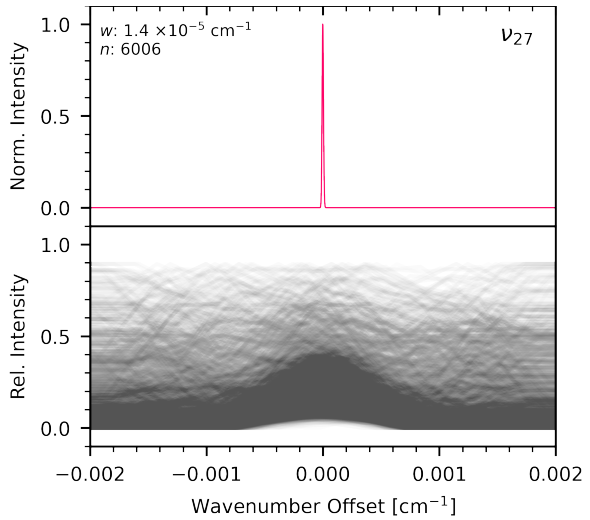

(b) ASAP^2 analysis for the ν_{27} band.

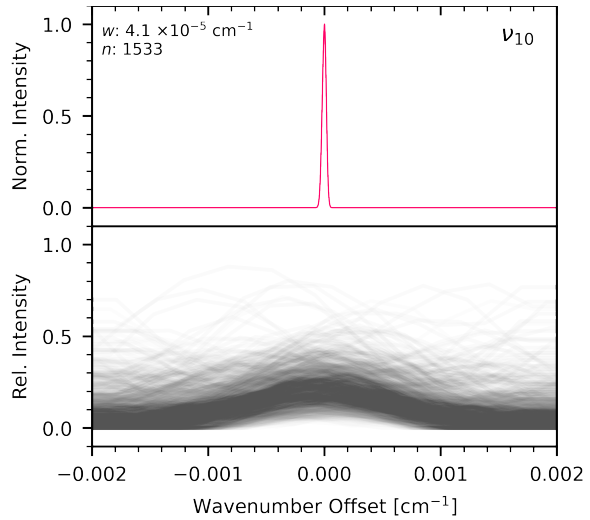

(c) ASAP^2 analysis for the ν_{10} band.

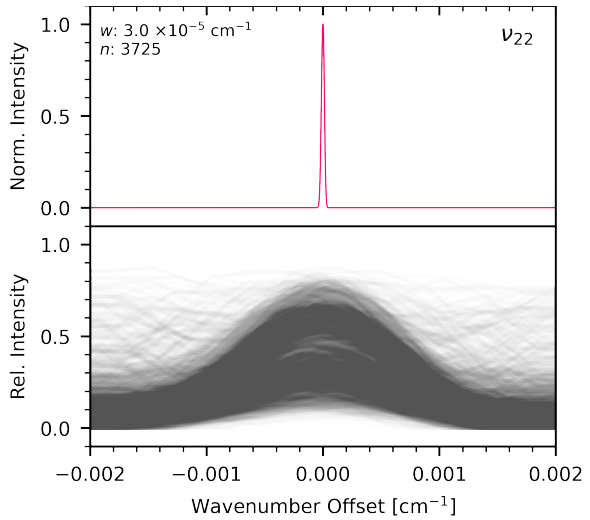

(d) ASAP^2 analysis for the ν_{22} band.

Figure S2: ASAP^2 cross-correlation peaks for the specified bands of cyclopentadiene (top) and their respective individual lines (bottom). In contrast to Fig. 5 of the main manuscript (and the other figures shown here), no saturated lines were excluded in (a). Comparison with Fig. 5 of the main manuscript shows that the influence on the center position is negligible.

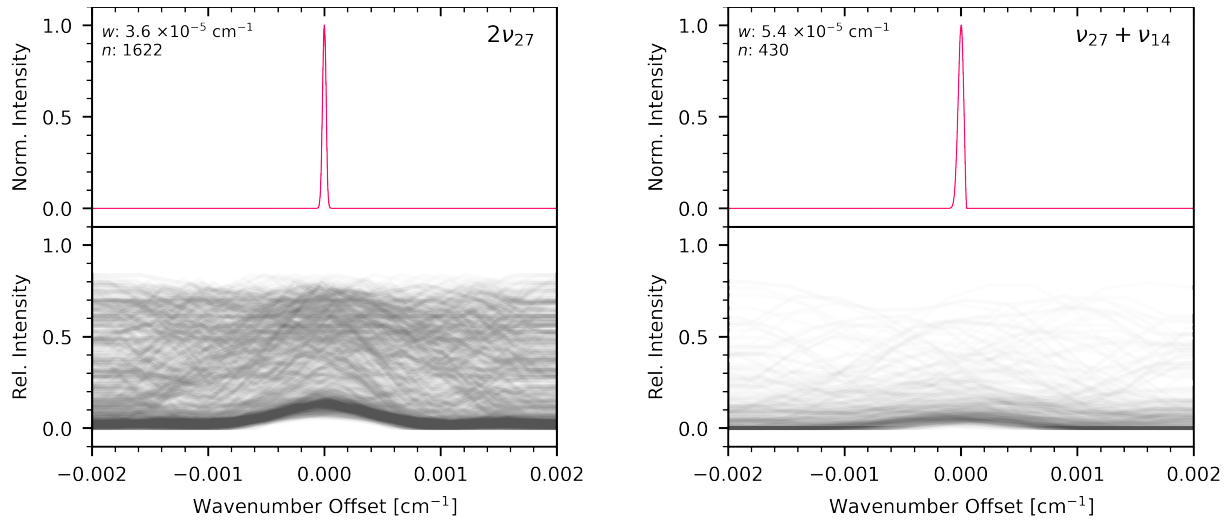

(a) ASAP^2 analysis for the $2\nu_{27} - \nu_{27}$ band.

(b) ASAP^2 analysis for the $\nu_{27} + \nu_{14}$ band.

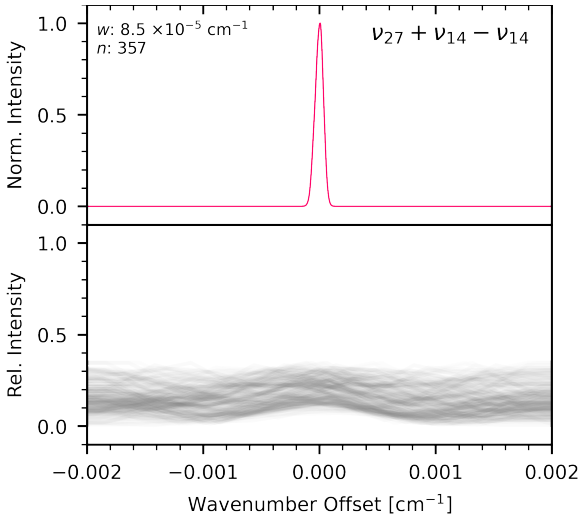

(c) ASAP^2 analysis for the $\nu_{27} + \nu_{14} - \nu_{14}$ band.

Figure S3: ASAP^2 cross-correlation peaks for the given bands of cyclopentadiene (top) and their respective individual lines (bottom).

in the main manuscript result from these excluded saturated lines. Omitting the saturated lines has only negligible effect on the resulting lineshape as can be seen by comparing Fig. 5 of the main manuscript (without saturated lines) and Fig. S2a (with saturated lines).

For all figures, intensities below 0 (due to the baseline correction) were set to exactly zero. This prevents an even number of negative intensities multiplying to a strong positive signal. However, a small artifact of the procedure can be seen in Fig. S3b where the right wing of the ASAP^2 peak is cut off due to the non-optimal baseline correction. Other options include using the absolute intensities and shifting up the whole spectrum by the noise floor. The optimal choice depends very much on the spectroscopic problem and the baseline correction. For our case, absolute intensities resulted in additional unwanted features to the

side of the peak. Shifting the spectrum by the noise floor eliminated the artifact but also increased the FWHM. As the uncertainty of the ASAP^2 analyses is typically dominated by the experimental uncertainty, this might be the preferred option for similar cases.

The lower half of the figures shows the intensities of the individual lines to highlight the different strengths of the different bands. Even very weak bands result in symmetric ASAP^2 peaks with high signal-to-noise ratios and narrow widths. For the bands presented here, the FWHMs of the ASAP^2 peaks range from $1.4 \times 10^{-5}\,\mathrm{cm}^{-1}$ for ν_{27} to $8.5 \times 10^{-5}\,\mathrm{cm}^{-1}$ for $\nu_{27} + \nu_{14} - \nu_{14}$. The FWHM is heavily tied to the number of cross-correlated transitions, see Fig. S5b.

C ASAP^2 in more detail

This section provides some more in-detail information on ASAP^2.

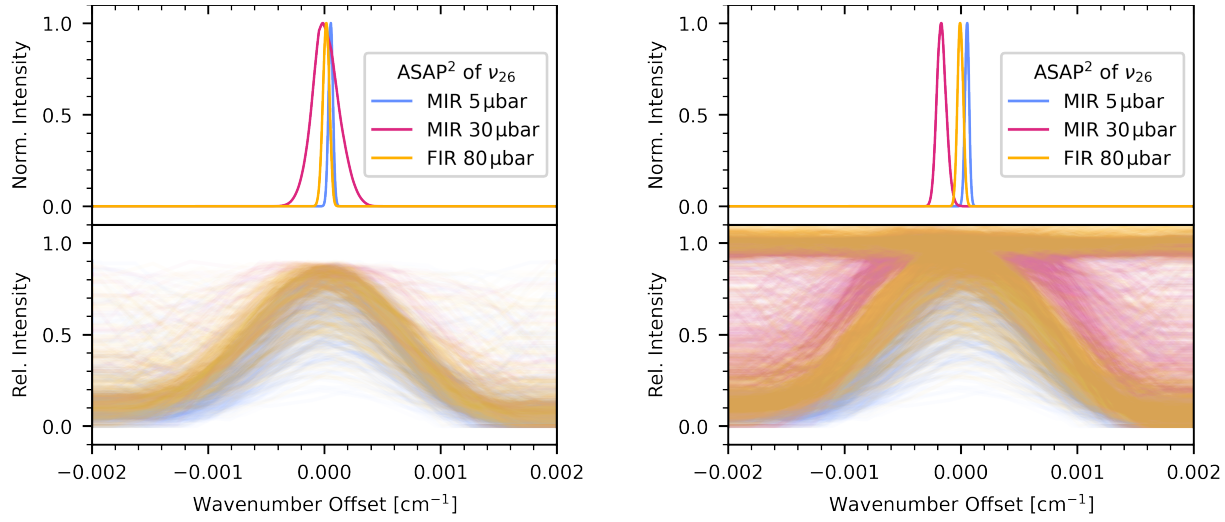

(a) Without saturated lines.

(b) All lines.

Figure S4: Cross-correlation peaks (top) and the individual lines (bottom) for the three different IR measurements of the ν_{26} band. In Figure (a) saturated lines were removed. There, the three peaks agree within about $1 \times 10^{-4}\,\mathrm{cm}^{-1}$ which is much smaller than the FWHM of the respective lines. In Figure (b), no lines were excluded, resulting in a worse agreement between the three cross-correlation peaks ($2.3 \times 10^{-4}\,\mathrm{cm}^{-1}$). Especially the lines from the 30 µbar spectrum are heavily saturated resulting in a shift of its cross-correlation peak.

First, the ASAP^2 analysis of the ν_{26} band at about $664\,\mathrm{cm}^{-1}$ is shown for the three different IR measurements in Fig. S4. The ν_{26} band was chosen as it is covered by all three IR measurements. Saturated lines (lines with a maximum intensity higher than 0.9) were excluded in Fig. S4a whereas all lines were used in Fig. S4b. The three resulting cross-correlation peaks are shown on top and the individual lines are shown in the bottom half. Both the widths and the center positions differ between the cross-correlation peaks for the different spectra. The varying widths are a result of the different pressures and for Fig. S4a

Table S1: The $P \times L$ values and number of unsaturated lines N_{Lines} for the three different spectra.

P [µbar]	L [m]	$P \times L$ [µbar · m]	N_{Lines}
5	140	700	1062
30	140	4200	101
80	25	1920	749

also of the different numbers of cross-correlated lines (as shown in Tab. S1). Higher $P \times L$ values increase the absorbance which leads to more saturated lines, which are filtered out in Fig. S4a. In contrast, all three spectra in Fig. S4b consist of $N_{\text{Lines}} = 1922$ individual lines.

The comparison between Fig. S4a and Fig. S4b shows that excluding the saturated lines is important. When removing the saturated lines, the center positions vary by about 1×10^{-4} which is well within the FWHM of the infrared lines (see the individual lines on bottom) and also of the same magnitude as the FWHMs of the cross-correlation peaks. With the saturated lines included, the agreement between the three cross-correlation peaks worsens, especially for the measurement with the highest $P \times L$ value, the MIR 30 µbar spectrum. Theoretically, saturated lines do not pose a problem as their intensity is constant over the cross-correlation peak. Multiplying the cross-correlation peak with a constant and subsequent renormalization results in the same cross-correlation peak. An explanation could be that the saturated lines are not perfectly constant but rather have a slight systematic slope. The root cause are probably artifacts from the baseline correction in combination with the saturated lines. Therefore it is recommended to use no or as-few-as-possible saturated lines for the best possible accuracy. This also highlights ASAP^2's vulnerability to systematic shifts which can come from saturation and baseline-correction effects (as shown here) but also from the wavenumber calibration.

We also tested the precision of ASAP^2 by repeating the analysis 100 times for randomly selected subsets of 10% of the total lines. The agreement between the cross-correlation peaks belonging to the same measurement (same colors) is very good (about $1 \times 10^{-4}\,\text{cm}^{-1}$, see Fig. S5a).

Last, Fig. S5b shows the progression of the cross-correlation peaks with the number of lines. They become narrower and more symmetric with increasing number of cross-correlated lines. At the same time, the differences between the cross-correlation peaks for 1000 and 2000 lines are very small indicating that the improvements diminish at some point.

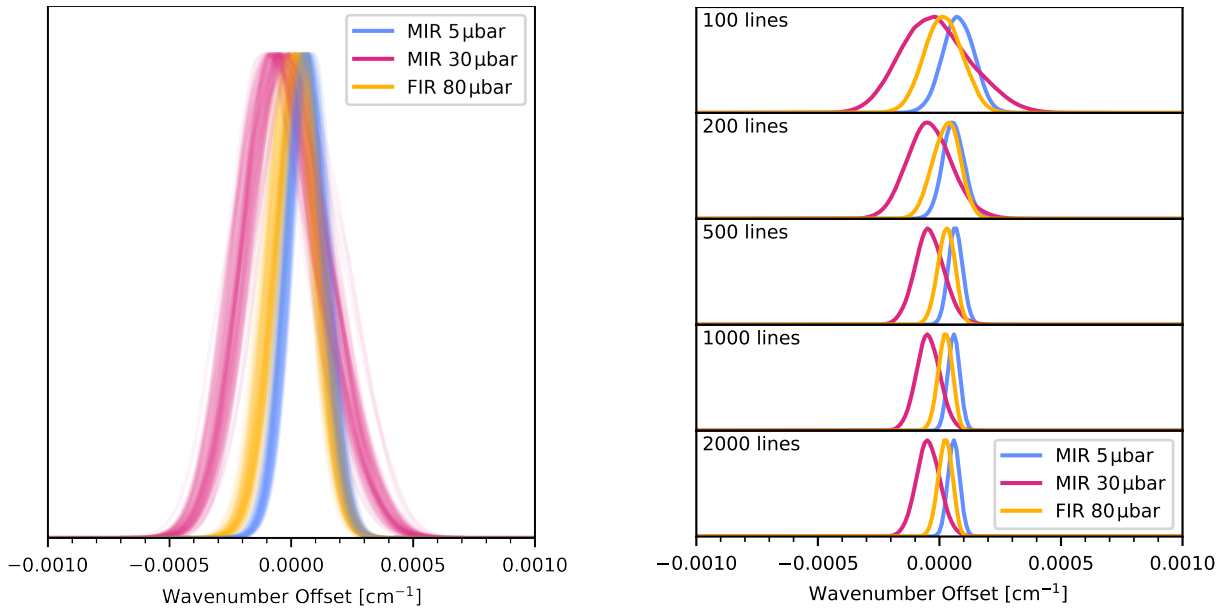

(a) (b)

Figure S5: ASAP^2 cross-correlation peaks of ν_{26} for 100 subsets each consisting of 10% of the total lines (a) and for different number of randomly selected lines (b).

References

(1) Bonah, L.; Helmstaedter, B.; Guillemin, J.-C.; Schlemmer, S.; Thorwirth, S. Extending the rotational spectrum of cyclopentadiene towards higher frequencies and vibrational states. J. Mol. Spectrosc. **2025**, 408, 111967.